BUBBLE PROPERTIES AND PRESSURE FLUCTUATIONS OF A SINGLE BUBBLE IN WATER

GYOUNG T. JIN AND SANG D. KIM
Department of Chemical Engineering, Korea Advanced Institute of Science and Technology, Seoul, 130-650 Korea

Key Words: Pressure Fluctuation, Pressure Spectrum, Bubble Size, Bubble Rising Velocity, Energy Dissipation Rate

The shape and rising velocity, pressure variation of a bubble and pressure spectrum from the pressure variation due to the rise of a bubble in water have been studied for bubble volumes from 1×10^{-6} to 5×10^{-5} m^3.

The vertical bubble length and radius of curvature are found to be 0.393 and 1.21 times the equivalent bubble diameter, respectively.

The mean frequency of the pressure spectrum decreases with increase in bubble size. The dynamic minimum pressure is related to the radius of curvature and the maximum pressure to the vertical bubble length. The pressure spectrum is correlated with the bubble properties.

The energy dissipation rate was determined from the pressure spectrum and was found to increase with increase in the bubble radius of curvature.

Introduction

Bubble properties (size, rising velocity and shape) can provide basic information for interpreting bubble characteristics in bubble columns and three-phase fluidized beds.

Pressure variation from a single bubble rising through a liquid is an important parameter for estimating bubble properties and the hydrodynamics around bubbles. Furthermore, the Fourier transform associated with such pressure variations can be used to evaluate bubble characteristics in bubble columns and three-phase fluidized beds by matching the Fourier transform of pressure fluctuations.[12]

Bubble properties in liquids have been studied on the basis of momentum balance, drag on wake behind a bubble, drag on bubble frontal area with its velocity and buoyancy force. The bubble shape,[3,4,10] rising velocity[1,5,8,20] and drag coefficient have been studied previously. In addition, studies of pressure variation in gas-fluidized beds[13,17,18,23] have received considerable attention. However, studies of pressure fluctuations of a single bubble in liquids are very few.

Therefore, in this study, pressure variation and bubble properties such as size, shape and rising velocity of a single bubble rising in water have been determined. Also, the rate of energy dissipation based on the pressure spectrum has been determined and compared with the values of Davies and Taylor.[8]

* Received September 18, 1989. Correspondence concerning this article should be addressed to S. D. Kim.

Theory

The surface pressure distribution over a spherical cap bubble has been described by Davies and Taylor[8] as

$$\frac{P_0-P_\theta}{\frac{1}{2}\rho U_b^2}=\frac{9}{4}\sin^2\theta \qquad (1)$$

where P_0, P_θ, ρ, and U_b are the pressure at the surface of a bubble nose and at the angle θ, density of liquid, and bubble rising velocity, respectively.

Bubble shapes have been expressed in terms of the Morton, Eötvös and Reynolds numbers.[3,10] Considering the wake behind a bubble, Collins[5,6] proposed a two-dimensional plane bubble as a bubble sink in a form of doublet in liquids. Simplifying the bubble shape as shown in **Fig. 1**, the following equation can be derived:

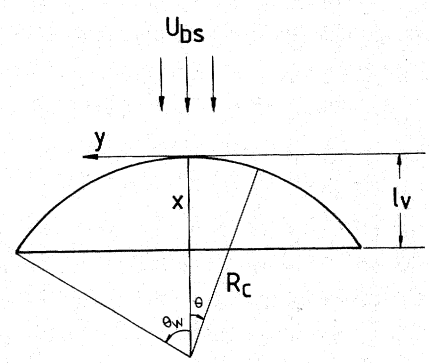

Fig. 1. Shape of a spherical cap bubble

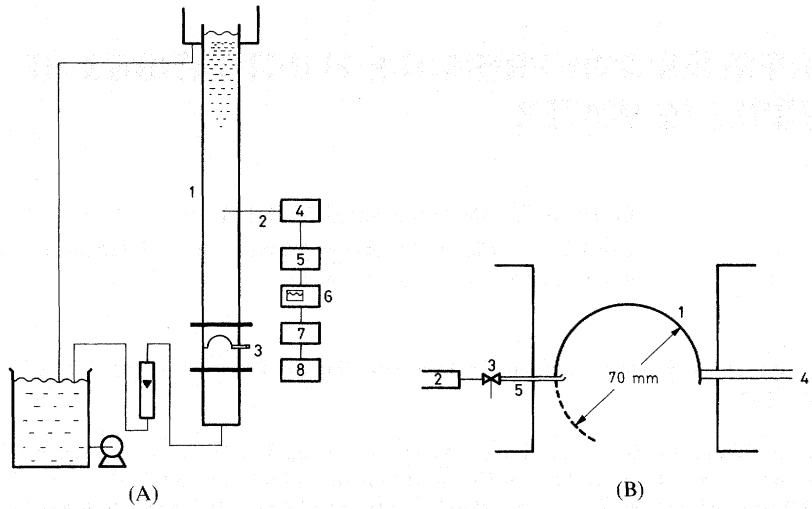

Fig. 2. Schematics of experimental apparatus
A) Overview: 1. main column 2. probe 3. bubble chamber 4. probe circuit 5. amplifier 6. oscilloscope 7. A/D converter 8. microcomputer
B) Bubble chamber: 1. hemisphere 2. syringe 3. three-way cock 4. rotating axis 5. needle

$$R_c = \frac{V + \frac{\pi}{3} l_v^3}{\pi l_v^2} \tag{2}$$

where R_c, l_v and V are the radius of curvature, the vertical bubble length and the volume of a bubble, respectively.

If pressure fluctuations are made up of the sum of signals with different frequencies, they can be analyzed by the Fourier transform. Since the pressure variation is known to be a function of bubble size, shape, rising velocity and wake properties, the bubble characteristics can also be determined from the Fourier transform.

The Fourier transform, $P(\omega)$, in the frequency domain is subject to the signal $P(t)$ in the time domain by

$$S_p(\omega) = \frac{1}{2\pi} \int_{-\infty}^{\infty} P(t)\, e^{-j\omega t}\, dt \tag{3}$$

The energy dissipation rate has been determined from the energy spectrum by Tennekes and Lumely[24] when its velocity fluctuations can be transformed by the Fourier transform.

The energy dissipation rate can be expressed as

$$\varepsilon = 2\nu \overline{s_{ij} s_{ij}} = 2\nu \int_0^{\infty} \omega^2 E(\omega) d\omega \tag{4}$$

where ν and s_{ij} are kinematic viscosity and shear stress, respectively.

Frost and Moulden[9] and Mazumdar[19] proposed a pressure spectrum which can be related to the energy spectrum, similarly to the relationship between the pressure and velocity fluctuations. The proposed relationship between the pressure and energy spectrums is given by Eqs. (5) and (6).

$$S_p(\omega) = k\rho^2 \omega E^2(\omega) \tag{5}$$

$$\int_0^{\infty} \omega^4 S_p(\omega) d\omega = \frac{12\rho^2}{5} \left[\frac{2}{3} \int_0^{\infty} \omega^2 E(\omega) d\omega \right]^2 \tag{6}$$

where constant k is 0.49 from the theory of Hinze[11] and 0.336 from the experiments of Batchelor.[2] These k values have been obtained from the relationship between the pressure and velocity fluctuations.

Another approach to determine the energy dissipation rate based on the drag force and the volume of wake behind a bubble in a liquid has been proposed by Davis and Taylor.[8]

Energy dissipation of a bubble is the product of mass and the rising velocity of a bubble. Thus, it would be proportional to the energy of buoyancy force[8]:

$$\varepsilon = C_D \pi A^2 \frac{1}{2} \rho U_B^2 U_B = g\rho V U_B \tag{7}$$

where C_D, A, U_B, and V are the drag coefficient, projected area, rising velocity and volume of a bubble, respectively.

1. Experimental

Experiments were carried out in a Plexiglas column of 0.1 m ID and 1.6 m height, as shown in **Fig. 2**. The main section of the column was constructed by flanging together two pieces of 0.1 m-ID × 0.8 m-high Plexiglas pipes. A rotatable hemispherical Plexiglas bubble chamber of 70 mm ID was placed at the center near the bottom of the column. A known volume of air was fed to the downfacing hemispherical chamber from a hypodermic needle with a syringe.

An electroresistivity probe was made of iron-constantan thermocouples as used by Park *et al.*[21]

The vertical distance between its two tips was 3 mm. The bubble probe was placed perpendicularly to the direction of bubble motion in order to reduce the interaction of bubbles with the probe.[22]

The bubble chamber was then flipped over so that a bubble was generated in the water column. As a bubble rose through the water column, the bubble properties and the mean pressure variation due to the bubble's rise in the column were measured at 0.6 m above the bubble chamber using an electroresistivity probe and a pressure transducer (PCB Elec. Co., 102A) with a power supplier and amplifier (PCB Elec. Co., 408) which measure the variation of absolute pressure due to a single bubble's rise in the column. The signals were observed by an oscilloscope and then amplified and stored in a microcomputer (Apple II) via an A/D converter. From these digitized data, bubble characteristics such as vertical bubble length, rising velocity[21] and pressure fluctuations were determined. The bubble volume was varied from 1×10^{-6} to $5\times10^{-5}\,m^3$.

From the bubble probe signals (**Fig. 3**), the bubble rising velocity, U_b, can be calculated from the following relation:

$$U_b=3\times10^{-3}/t_1 \tag{8}$$

where t_1 is the time delay between the corresponding pulses in the two channels of the recorded data.

The vertical bubble length, l_v, can be determined from the signal with the following relation:

$$l_v=t_2\times U_b=3\times10^{-3}(t_2/t_1) \tag{9}$$

where t_2 is the pulse width in the unit of time in the signal.

To compare the bubble size from the bubble probe and that from the still photographic measurements, the bubbles in a two-dimensional acrylic column (0.025 m thickness × 0.44 m width × 1.8 m height) were measured by the probe and photographic methods. It was found that the bubble sizes were determined by the photographic method are slightly larger than those determined by the probe method, but the difference is less than 10%.

2. Results and Discussion

Typical response curves of variations in dynamic pressure and in electroresistivity due to a bubble rising in water are shown in Fig. 3. In general, the output signals have same general shapes with good reproducibility. From the electroresistivity signals, the bubble chord length, l_v, and its rising velocity, U_b, have been determined[21] from Eqs. (8) and (9). Also, bubble shape in terms of the radius of curvature has been determined from Eq. (2) with the knowledge of bubble length and volume.

The pressure variation with time exhibits a maximum and a minimum dynamic pressure. When a bubble reaches the probe, the maximum pressure is obtained at the nose of a bubble. While a minimum pressure is obtained at the center of the wake (Fig. 3), however, the reason why a minimum pressure appears at the center of the wake is not clear.[16]

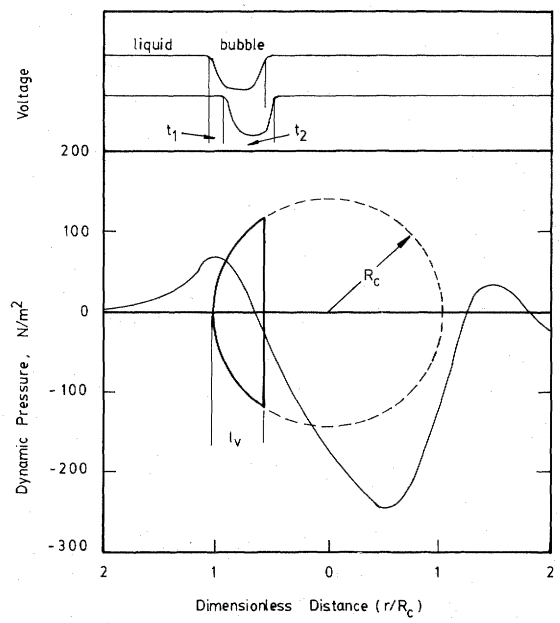

Fig. 3. Typical pressure and resistivity signals during a single bubble rise (bubble volume = $1\times10^{-6}\,m^3$)

2.1 Bubble shape

The shape of the equivalent diameter of a bubble exceeding 12 mm is observed to be a spherical cap with an open unsteady wake in the present experimental conditions[10] on the basis of the bubble shape classification of Bhaga and Weber.[3]

Bubble shape in terms of the radius of curvature and vertical length is shown as a function of bubble diameter in **Fig. 4**. As can be seen, the radius of curvature and the vertical bubble length increase with increase in equivalent bubble diameter. If a bubble shape is spherical, the radius of curvature should be half of the equivalent diameter. However, the radius of curvature is found to be approximately 1.21 times the equivalent diameter of the same bubble volume of the spherical cap shape.

The relationship between bubble shape and equivalent bubble diameter has been obtained as:

$$l_v=0.393\,d_e \tag{10}$$

with a correlation coefficient of 0.988. Also, the relationship between R_c and d_e can be derived from Eqs. (2) and (10) with the known volume of a bubble as:

$$R_c=1.210\,d_e \tag{11}$$

It has been reported that the wake angle, θ_w, for a spherical cap bubble in a Newtonian liquid depends

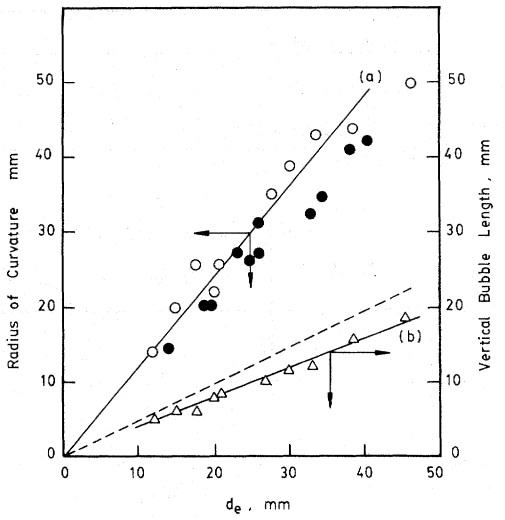

Fig. 4. Relationships between equivalent bubble diameter and curvature of radius (a) and vertical bubble length (b) ●: Davies and Taylor (1950), ○: present data of R_c, △ present data of l_v, ---- spherical bubble

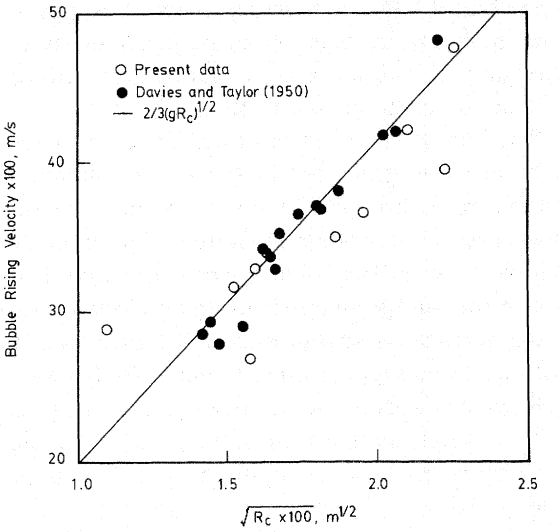

Fig. 5. Relationship between bubble rising velocity and radius of curvature

on the bubble Reynolds number[4] and is represented empirically by

$$\theta_w = 50 + 190 \exp(-0.62\, Re_b^{0.4}) \qquad (12)$$

where Re_b is the bubble Reynolds number. In the present study, Re_b is greater than 3000, for which condition the above equation gives $\theta_w = 50$ degrees with sufficient accuracy. On the other hand, according to Fig. 1, $\tan\theta_w$ and substituting R_c of Eq. (11) and l_v of Eq. (10) gives $\tan\theta_w = 1.09$, hence $\theta_w = 48$ degrees. This accords well with the prediction from Eq. (12).

2.2 Rise velocity

Bubble rising velocity is a function of buoyancy, gravitational, drag, and surface tension forces. These forces may dissipate to the drag on the bubbles, momentum of the rising bubbles and that of the wakes.[6]

A theroretical model of a rising bubble as a function of the radius of curvature has been proposed by Davies and Taylor,[8] using the surface pressure distribution over a spherical bubble as

$$U_{bs} = k\sqrt{gR_c} \qquad (13)$$

where k is 2/3 and R_c is the radius of curvature.

The relationship between the bubble rising velocity and the radius of curvature is shown in **Fig. 5**. In the figure, the experimental values of the present study and of Davies and Taylor[8] are compared with the theoretical values from Eq. (13). As can be seen, the bubble rising velocity increases with increase in the radius of curvature according to Eq. (13). However, when the radius of curvature is greater than 11 mm, the rising velocity exhibits lower values than that of the theoretical ones since bubble size larger than 12.5 mm in diameter in the present experimental apparatus may exhibit the wall effect.[49] As can be observed, the spherical cap shaped bubbles agree quite well with the theoretical values of Eq. (13). However, the shape changes from oblate to spherical cap when the bubble diameter exceeds about 12 mm[10] as observed in the present study. Under these conditions, the observed bubble rising velocity begins to deviate from the above model as the radius of curvature becomes 1.21 times the bubble diameter (Eq. 11). When the bubble volume exceeds 1×10^{-6} m^3, the rising velocity exhibits somewhat higher values than those from Eq. (13) since the observed bubble shape is ellipsoidal rather than spherical cap.[10]. Based on an approximate predictive equation of Wallis,[4] the bubble rising velocity of maximum bubble size (45.6 mm) would be reduced about 28% compared to the bubble rise velocity in an infinite space.

2.3 Pressure variation

Dynamic pressure is found to be high at the bubble nose and low at the bubble wake. The field of minimum pressure has been observed at the center of the wake. Similar results have been observed around two dimensional bubbles in a gas-fluidized bed by Lirag and Littman.[16]

The positions of minimum pressure as a function of the radius of curvature and of the maximum pressure as a function of the vertical bubble length are calculated from the product of the time lag (ΔT) from the maximum to minimum pressures and a single bubble rising velocity (U_{bs}) as shown in **Fig. 6** in which the solid and dashed lines represent the values corresponding to the bubble nose, l_v, and the center of the wake, $(2R_c - l_v)/2$ from the bottom of a bubble, respectively.

The dynamic pressure variations with the equivalent bubble diameter are shown in **Fig. 7**. The obtained

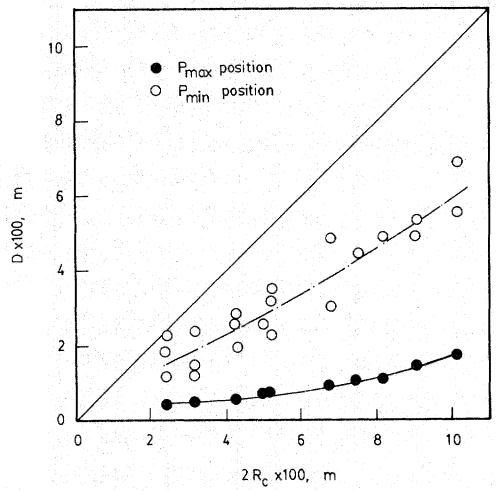

Fig. 6. Position of the maximum and minimum dynamic pressure during a single bubble rise in water

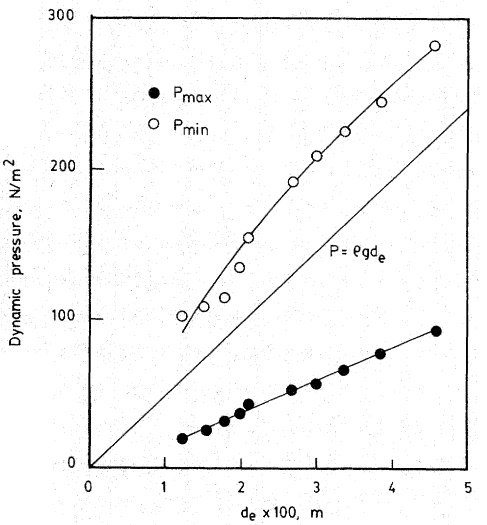

Fig. 7. Relationship between maximum and minimum pressure change and equivalent diameter

maximum and minimum pressures are lower and higher than those from the equation ($P=\rho g d_e$) of Davidson.[7] This may be due to the fact that the Davidson's model assumes the bubbles in a gas-fluidized bed to be spherical in shape. However, the bubbles in liquids is very close to a spherical cap shape. Bubbles in liquids may have a large wake with large amount of eddies. Therefore, the ratio of minimum to maximum pressures is in the range of 3 to 5. The maximum pressure on the bubble nose is the potential energy that may move liquid downward which may affect the vertical bubble length. However, the minimum pressure seems to be affected by the wake and its size is related to the radius of curvature. Therefore, the dynamic maximum pressure could be related to the vertical bubble length and dynamic minimum pressure to the radius of curvature in terms of the following relevant dimensionless term as shown

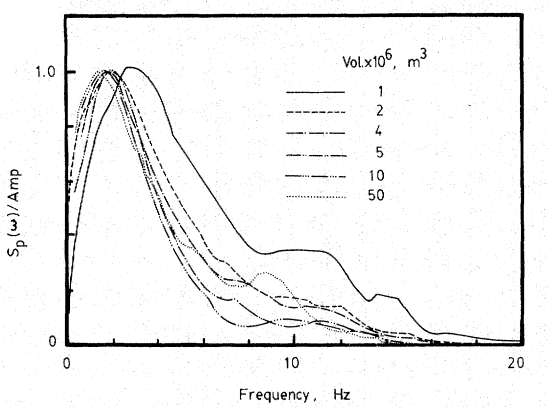

Fig. 8. Pressure spectrum of a single bubble rise in water

in Eqs. (14) and (15).

$$P_{\max} = +0.566\,\rho g l_v \tag{14}$$

$$P_{\min} = -0.566\,\rho g R_c \tag{15}$$

where + and − denote the positive and negative pressure fields, respectively (Fig. 2). Also l_v is the vertical bubble length; R_c is the radius of curvature, respectively.

2.4 Pressure spectrum

The pressure spectrum of a single bubble is shown in **Fig. 8**. If the signal is a sine function, its spectrum has a peak at a given frequency. Since the present signals have multiple frequencies, their pressure spectrum can be obtained from the discrete Fourier transform.[16] Since the time lag between the maximum and minimum pressures is a function of the velocity and the radius of a bubble, the main frequency in the pressure spectrum can be expressed as the reciprocal of the time lag.

$$\omega_{\text{main}} = \frac{1}{2\Delta T} \tag{16}$$

where ΔT is the time lag from maximum to minimum pressures.

The time lag should be a function of the vertical bubble length, the radius of curvature and the rising velocity. Assuming that the pressure change can be represented by the model of Davidson[7] and the velocity by the model of Davies and Taylor,[8] the present frequency can be represented by

$$\omega = \frac{U_{bs}}{4R_c} = \frac{1}{6}\sqrt{g/R_c} \tag{17}$$

The frequency between the main frequency of the pressure spectrum and the radius of curvature is shown in **Fig. 9**. As can be seen, the peak frequency obtained from the time lag (Eq. 16) is higher than that from Eq. 17.[7] Therefore, the bubble characteristics cannot be determined from a peak frequency alone. Also, the peak frequency from the pressure spectrum is found

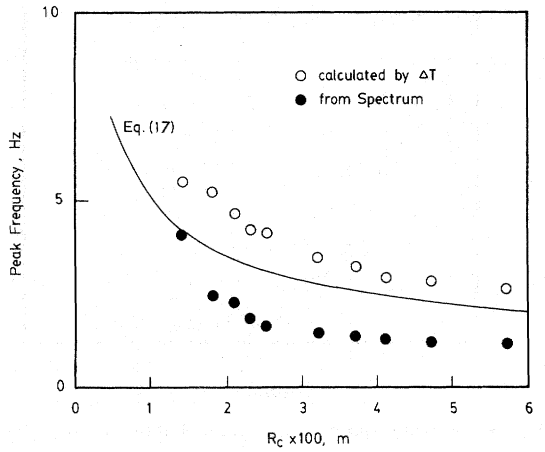

Fig. 9. Relationship between radius of curvature and peak frequency
○: calculated from ΔT (equation 12), ●: calculated from the spectrum

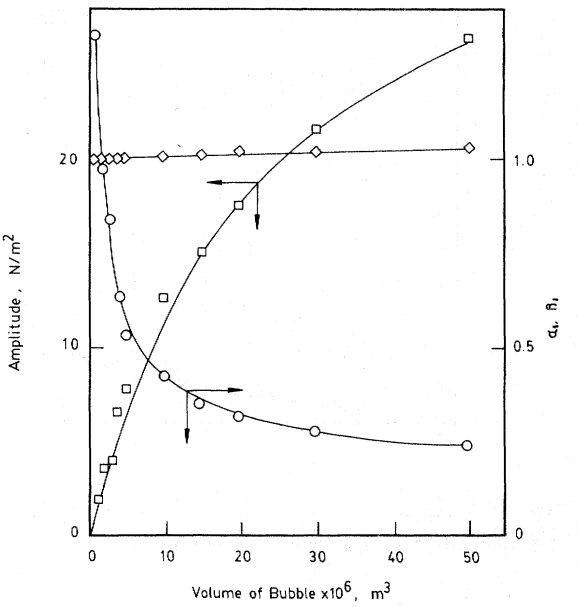

Fig. 10. Relationships between bubble volume and amplitude of pressure spectrum and mean and standard deviation of pressure spectrum
□: A_{mp}, ○: α_1, △: β_1

to be lower than that calculated from Eq. 17.[7] Thus, the bubble properties should be determined from the pressure spectrum of a single bubble (Fig. 8) from which the bubble properties in bubble columns and three-phase fluidized beds can be deduced.

To determine the pressure spectrum of a single bubble, the relationship between the frequency of pressure spectrum, $S_p(\omega)$, and its amplitude, A_{mp}, is needed. Such a relationship has been correlated with the bubble properties (**Fig. 10**) of the present study as:

$$S_p(\omega)=A_{mp}\exp\left[-\frac{(\ln\omega-\alpha_1)^2}{\beta_1^2}\right]^2 \qquad (18)$$

where

$$A_{mp}=1.535\,d_e^{2.00}$$
$$\alpha_1=1.865\,d_e^{-1.40}$$
$$\beta_1^2=1.10$$

in which α_1 and β_1 are the mean and standard deviation of the pressure spectrums, respectively.

In general, the time lag between the minimum and maximum pressures is proportional to the square root of the bubble radius. Large bubbles have low peak frequency in the pressure spectrum.

2.5 Energy dissipation rate

The energy dissipation rates obtained from Eqs. (4) and (7) are shown in **Fig. 11**. Since the energy dissipation rates from the above equations are based on the whole bubble volume, the frontal area of a bubble has been multiplied to the energy dissipation rate from the pressure spectrum.[9]

Since the pressure signal varies along the vertical axis of a bubble, the bubble length is an indicator of the energy dissipation rate in the pressure spectrum. Also, the energy dissipation rates have been used to interpret the mass and heat transfer mechanisms in

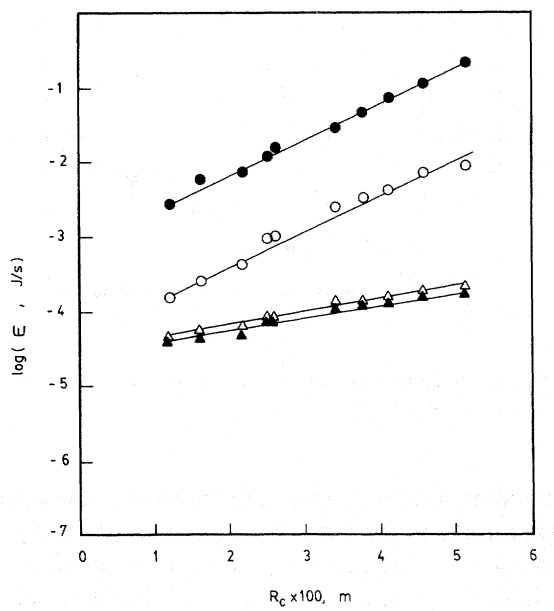

Fig. 11. Relationship between radius of curvature and energy dissipation rate in water
● from Eq (7) [Davis and Taylor[8]]
○ from $A_f\,\varepsilon$ [Frost and Moulden[9]]
△ from ε [Frost and Moulden[9]]
▲ from ε [Mazumdar[19]]

fluidized beds.[14,15] Therefore, the energy dissipation rate of a single bubble can be extended to the multibubbles in bubble columns and three-phase fluidized beds to estimate the bed hydrodynamics, mass and heat transfers.

The energy dissipation rate obtained from the pressure spectrum is lower than that obtained from

Eq. (7) based on the drag coefficient. The difference can be attributed to the way of determining the bubble volume and the bubble frontal area.

The relationship between the energy dissipation rate and the radius of curvature on the basis of drag coefficient is as follows.

$$\varepsilon = 0.2\, g^{1.5} \rho R_c^{3.5} \tag{19}$$

As can be seen, the energy dissipation rate is well represented by the radius of curvature (Fig. 11). However, the dissipation rate based on the drag coefficient is found to be about twice that based on the bubble frontal area.[9]

It is known that the viscous forces mainly govern energy dissipation in small-scale eddies. Prior to energy dissipation, the energy is transferred from a large to a smaller eddy. With this transfer mechanism, the energy transfer or dissipation may contribute to the mass and heat transfer in bubble columns and three-phase fluidized beds. The overall energy dissipation rate of a bubble has been proposed by Davies and Taylor.[8] However, their values are much higher than those from the pressure spectrum[9,19] (Fig. 11). This difference may be due to the instability of the wake since the energy dissipation is related to the momentum balance and the instability of bubbles which may affect the bubble rising velocity. However, pressure variation due to the eddy motion is more important than the instability. Nonetheless, the energy dissipation rate increases with increase in radius of curvature. Since energy dissipation based on the drag includes the energy production term, energy dissipation in the bubble can be characterized by the bubble size which affects small-scale eddies.

Conclusions

The rising velocity of bubbles of more than 12 mm in diameter and of spherical cap shape is well represented by the equation of Davies and Taylor.[8] The vertical bubble length is 0.393 times the equivalent bubble diameter and the radius of curvature is approximately 1.21 times the equivalent bubble diameter. Dynamic maximum and minimum pressures have been observed at the bubble nose and the center of the wake, and these values have been correlated with a dimensionless term in Eqs. (14) and (15). The main frequency of pressure spectrum of a single bubble decreases with increase in bubble size. The pressure spectrum of a single bubble can be correlated with the equivalent bubble diameter according to equation (18). The energy dissipation rate from the pressure spectrum is found to have a similar trend to that of Davies and Taylor.[8] This rate can be correlated with the radius of curvature and liquid density by equation (19).

Acknowledgement

The financial support for this work from the Korea Science and Engineering Foundation is gratefully acknowledged.

Nomenclature

A	=	projected area of a bubble	[m^2]
A_f	=	bubble frontal area	[m^2]
A_{mp}	=	amplitude of pressure spectrum	[N/m^2]
C_D	=	drag coefficient	
d_e	=	equivalent bubble diameter	[m]
D	=	distance between maximum and minimum pressures in a single bubble	[m]
$E(\omega)$	=	energy spectrum	
g	=	gravitational acceleration	[m/s^2]
j	=	complex variable	
k	=	proportional constant in Eq. (5)	
l_v	=	vertical bubble length	[m]
$P(t)$	=	transient pressure response	[N/m^2]
P_{max}	=	dynamic maximum pressure	[N/m^2]
P_{min}	=	dynamic minimum pressure	[N/m^2]
P_0	=	pressure at nose of bubble	[N/m^2]
P_θ	=	pressure at angle θ	[N/m^2]
r	=	radial distance	[m]
R_c	=	radius of curvature of bubble	[m]
R_{eb}	=	bubble Reynolds number	
s_{ij}	=	stress	[N/m^2]
$S_p(\omega)$	=	pressure spectrum related to energy spectrum	[N/m^2]
t	=	time	[s]
t_1	=	time delay between corresponding pulses in the two channels of recorded data	[s]
t_2	=	pulse width in the unit of time in the bubble signal	[s]
ΔT	=	time difference between maximum and minimum in the pressure-time curve	[s]
U_b	=	bubble rising velocity	[m/s]
U_{bs}	=	single-bubble rising velocity	[m/s]
V	=	volume of bubble	[m^3]
x	=	Cartesian coordinate	[—]
y	=	Cartesian coordinate	[—]
α_1	=	logarithmic mean of pressure spectrum	[N/m^2]
β_1	=	logarithmic standard deviation of pressure spectrum	[N/m^2]
ρ	=	density	[kg/m^3]
μ	=	viscosity	[Pa/s]
ν	=	kinematic viscosity	[m^2]
ε	=	energy dissipation rate	[J/s]
σ	=	surface tension	[N/m]
θ	=	angle	
θ_w	=	wake angle	
ω	=	frequency	[Hz]

Literature Cited

1) Angelino, H.: *Chem. Eng. Sci.* **17**, 87 (1966).
2) Batchelor, G. K.: "*An Introduction to Fluid Dynamics*", Cambridge Univ. Press (1967).
3) Bhaga, D. and M. E. Weber: *J. Fluid Mech.* **105**, 85 (1981).
4) Clift, R., J. R. Grace and M. E. Weber: "*Bubbles, Drops and Particles*", Academic Press, New York (1978).
5) Collins, R.: *J. Fluid Mech.* **22**, 763 (1965).
6) Collins, R.: *Chem. Eng. Sci.* **26**, 90 (1967).
7) Davidson, J. F. and D. Harrison Eds.: "*Fluidization*", Academic Press, New York (1971).

8) Davies, R. M. and Sir. G. Taylor: *Proc. Royal Soc.* **A200**, 375 (1950).
9) Frost, W. and T. H. Moulden: "*Handbook of Turbulences*", Plenum Press, New York (1977).
10) Grace, J. R.: *Trans. Instn. Chem. Engrs.* **51**, 116 (1973).
11) Hinze, O.: "*Turbulence*", McGraw-Hill, New York. (1959).
12) Jin, G. T.: "The Characteristics of Bubbles and Pressure Fluctuations in Bubble Columns and Three-Phase Fluidized Beds", Ph. D. Thesis, KAIST, Seoul, Korea (1985).
13) Kato, T., S. Mori and I. Muchi: *Kagaku Kogaku Ronbunshu*, **2**, 109–114 (1976).
14) Kato, Y., K. T. Uchida, T. Kago and S. Morooka: *Powder Technol.* **28**, 173 (1981).
15) Lamont, J. C. and D. S. Scott: *AIChE J.* **16**, 513 (1970).
16) Lirag, R. C. and H. Littman: *AIChE Symp. Ser.* **67** (116), 11 (1971).
17) Littman, H. and G. A. J. Homolka: *Chem. Eng. Prog. Symp. Ser.* **66** (105), 37 (1970).
18) Littman, H. and G. A. J. Homolka: *Chem. Eng. Sci.* **28**, 2231 (1973).
19) Mazumdar, H. P.: *App. Sci. Res.* **35**, 367 (1979).
20) Mendelson, H. D.: *AIChE J.* **13**, 250 (1967).
21) Park, W. H., W. K. Kang, C. E. Capes and G. L. Osberg: *Chem. Eng. Sci.* **24**, 851 (1969).
22) Rowe, P. N. and H. Masson: *Trans. Instn. Chem. Engrs.* **59**, 177 (1981).
23) Stewart, P. S. B.: *Trans. Instn. Chem. Engrs.* **46**, T60 (1968).
24) Tennekes, H. and J. L. Lumley: "A First Course in Turbulence", MIT Press, 263 (1973).